Models of Eukaryotic Gradient Sensing: Application to Chemotaxis of Amoebae and Neutrophils

Andre Levchenko* and Pablo A. Iglesias†

*Divisions of Biology, California Institute of Technology, Pasadena, California 91125 and †Department of Electrical and Computer Engineering, Johns Hopkins University, 105 Barton Hall, Baltimore, Maryland 21218 USA

ABSTRACT Eukaryotic cells can detect shallow gradients of chemoattractants with exquisite precision and respond quickly to changes in the gradient steepness and direction. Here, we describe a set of models explaining both adaptation to uniform increases in chemoattractant and persistent signaling in response to gradients. We demonstrate that one of these models can be mapped directly onto the biochemical signal-transduction pathways underlying gradient sensing in amoebae and neutrophils. According to this scheme, a locally acting activator (PI3-kinase) and a globally acting inactivator (PTEN or a similar phosphatase) are coordinately controlled by the G-protein activation. This signaling system adapts perfectly to spatially homogeneous changes in the chemoattractant. In chemoattractant gradients, an imbalance between the action of the activator and the inactivator results in a spatially oriented persistent signaling, amplified by a substrate supply-based positive feedback acting through small G-proteins. The amplification is activated only in a continuous presence of the external signal gradient, thus providing the mechanism for sensitivity to gradient alterations. Finally, based on this mapping, we make predictions concerning the dynamics of signaling. We propose that the underlying principles of perfect adaptation and substrate supply-based positive feedback will be found in the sensory systems of other chemotactic cell types.

INTRODUCTION

Many biological systems have the ability to sense the direction of external chemical sources and respond by polarizing and migrating toward chemoattractants or away from chemorepellants. This phenomenon, referred to as chemotaxis, is crucial for proper functioning of single-cell organisms, such as bacteria and amoebae, and multi-cellular systems as complex as the immune and nervous systems. Chemotaxis also appears to be important in wound healing and tumor metastasis. A common feature of most chemotactic signaling systems is the ability to adapt to different levels of external stimuli, so that it is the gradient of signaling molecule rather than the average signal value that determines the response. Chemotactic cells exhibiting perfect adaptation respond to spatially homogeneous increases in external stimulus by transient activation of specific intracellular signaling pathways. The same signaling pathways, however, can be activated persistently if the signal is presented in a spatially inhomogeneous, graded manner. The goal of this analysis is to extend our understanding of these processes by creating a single model explaining both adaptation and gradient sensing.

The need for chemotaxis presents cells with a daunting problem of detecting often exceedingly shallow and changing gradients of extracellular substances and regulating a complex locomotion apparatus to move in accordance with the direction and the value of these gradients. The mechanism for attaining a highly complex and integrated response such as this calls for an explanation and modeling in quantitative rather than qualitative terms. Mathematical and computational modeling can provide a translation of seemingly logical biochemically-based arguments into a set of predictions of dynamical and steady-state properties of the system. Using mathematical formalism, alternative hypotheses can be contrasted more easily and criteria found for discarding a hypothesis-contradicting experimental observations, sometimes in a subtle and counterintuitive way. In addition, mathematical models can provide insight into some general design principles that biochemically-based cell control systems can use to perform a particular function. All these considerations are especially true for the intricate regulation of eukaryotic gradient sensing and chemotaxis, leading to a long history of a quantitative and modeling research.

Our model attempts first to derive principles that must be true for any chemotactic cell capable of displaying both perfect adaptation and persistent signaling with nonlinear signal amplification, and then, to investigate whether and how these principles are effected in a particular cell system. As a result, we will obtain a model related to a simple mechanism for gradient sensing, qualitatively outlined recently (Parent and Devreotes, 1999), thus providing support for some of its premises and conclusions, but also making the model more realistic and quantitative. We then complement it with a new mechanism for signal amplification and show how this model can be experimentally verified. We also argue that an alternative hypothesis for a mechanism of gradient sensing outlined in the next paragraph is probably invalid, at least in amoebae and neutrophils. The dynamical

Received for publication 23 April 2001 and in final form 11 October 2001.

Dr. Levchenko's present address is Dept. of Biomedical Engineering, Johns Hopkins University, Baltimore, MD 21218.

Address reprint requests to Pablo Iglesias, Dept. of Electrical and Computer Engineering, Johns Hopkins University, 105 Barton Hall, 3400 N. Charles St., Baltimore, MD 21218. Tel.: 410-516-6026; Fax: 410-516-5566; E-mail pi@jhu.edu.

0006-3495/02/01/50/14 $2.00

model presented in our study can thus provide a mathematical formalism that can be used more effectively as a paradigm of eukaryotic gradient sensing.

Unlike most explanations of eukaryotic gradient sensing presented to date, the phenomenological model put forward in Meinhardt (1999) is formulated mathematically and results in semiquantitative predictions. This model is based on the principle, formulated by Turing and adapted in Gierer and Meinhardt (1972) to explain biological pattern formation. The Turing principle postulates that stable patterns may arise if there is an autocatalytic local production of an activator that also causes production of an inhibitor. Unlike the activator, the inhibitor is assumed to be capable of long-range diffusion. This model is based on local positive and global negative feedback that can lead to a substantial amplification of a locally applied signal, thus making it attractive in trying to account for substantial signal amplification observed in eukaryotic gradient sensing. However, in addition to predicting signal amplification, the Turing principle also predicts that the activation pattern becomes stable. This presents a problem, because it is known that the gradient-sensing signaling systems need to readjust themselves continuously to be able to sense changes in the environment. In Meinhardt (1999), this difficulty is overcome by proposing a second inactivating enzyme with a longer activation time, acting locally to "poison" the activity peak and "unlock" the local activation in the system. This assumption however makes the model far less parsimonious and, thus, more difficult to accept.

Meinhardt also points out that the cytoskeleton rearrangements are integral to biochemical interpretation of his model. Recently, it has been realized, however, that eukaryotic gradient sensing can be decoupled from cytoskeleton-dependent processes. In particular, *Dictyostelium discoideum* cells, in which actin polymerization is inhibited by latrunculin A, can still activate a variety of signaling pathways in a gradient-dependent, spatially polarized manner (Parent and Devreotes, 1999). These rounded cells, lacking mobility and polarization imposed by actin polymerization, clearly exhibit both adaptability and persistence of signaling without substantial dynamic fluctuations observed in cells with intact actin polymers. It can be demonstrated that Meinhardt's model fails to account for this behavior. In particular, the model predicts no perfect adaptation, whereas action of the two inhibitors make persistent activation at a particular membrane location impossible. Finally, it should be pointed out that the phenomenon of the Ca^{2+}-induced Ca^{2+} release from the intracellular stores postulated as the mechanism of the positive feedback is doubtful, because inhibition of Ca^{2+} concentration changes by cell permealization and other means does not affect gradient sensing in *D. discoideum*, a common model system used in studies of eukaryotic chemotaxis (Van Duijn and Van Haastert, 1992; Traynor et al., 2000). Several studies suggested that the only aspect of chemotaxis for which upregulation of Ca^{2+} is required is efficient detachment of the uropode in migrating amoebae and neutrophils (Eddy et al., 2000). These considerations call into question the general applicability of the approach in Meinhardt (1999) to modeling of gradient sensing.

Decoupling chemoattractant gradient sensing from cell movement and cytoskeletal rearrangements can greatly facilitate consideration of the underlying biochemical regulation. Indeed, the actin cytoskeleton remodeling and its connection to various intracellular and extracellular cues mediated by a multitude of regulatory proteins may present an intimidating if not impossible task for a modeler. The matter is further complicated by the need to account for cell adhesion properties, loss and synthesis of the cell membrane, variable cell shape, etc. It is therefore of importance that gradient sensing and cytoskeleton regulation represent separable components of chemotaxis. In this work, we concentrate on the analysis of the cytoskeleton-independent gradient sensing, creating a model that may be integrated with the model of cytoskeletal regulation at a later point.

We present, here, necessary conditions for the organization or topology of a gradient-sensing biochemical network and a plausible biochemical scheme that may embody these principles in *D. discoideum* and neutrophils. Whereas the models by Meinhardt and others (D. Lauffenburger and A. Arkin, personal communications) were driven primarily by the need to explain high gain in gradient sensing, we use a different strategy. It consists in accounting first for perfect adaptation (because it does not involve spatial consideration, and the model is simpler), then in seeing how this model needs to be modified to account for persistent signaling, as opposed to adaptation, in the presence of gradients. Finally, we explore possible mechanisms of signal amplification consistent with adaptation and persistent signaling.

MODEL AND RESULTS

Perfect adaptation to spatially uniform changes in ligand concentrations

Perfect adaptation is commonly observed in gradient-sensing systems (Alon et al., 1999; Van Haastert, 1983). A simple analysis shows that perfect adaptation allows a sensory system to respond to the gradient itself rather than to the absolute value of the signal. Any deviation from the precise character of adaptation can result in persistent activation in the absence of signal gradients, a situation that can severely limit the range of inputs, over which a system can operate efficiently. We thus need to account for perfect adaptation in our model of gradient-sensing signal transduction.

A mechanism for generating robust perfect adaptation based on receptor modification has been proposed previously for bacterial chemotaxis (Alon et al., 1999; Yi et al., 2000). However, receptor modification has been shown to

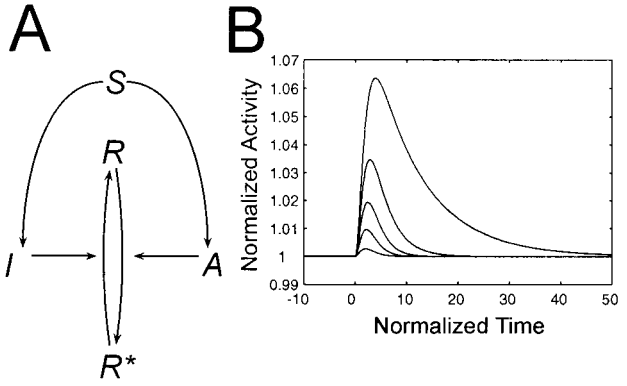

FIGURE 1 Scheme for achieving perfect adaptation. (*A*) The response element can be found in one of two states: active (*R**) or inactive (*R*). Transitions between the two states are catalyzed by the activation (*A*) and inactivation (*I*) enzymes. The activity levels of the two enzymes are both regulated by the signal (*S*). (*B*) Sample predictions of the adaptation scheme depicted in (*A*). Normalized concentration of the response element is plotted as a function of normalized time for a 10% increase at time 0 in the concentration of the signaling molecule *S*. The ratio α of inactivation rates of *I* and *A* determines the transients. For $0 < \alpha < 1$, activation of *A* is faster than that of *I*, resulting in a transient increase in the concentration of *R**. Smaller values of α lead to larger transients and longer adaptation times. Plots corresponding to values of α of 0.1 (largest transient) 0.3, 0.5, 0.7 and 0.9 (smallest transient) are shown.

be unessential for G-protein-mediated adaptation in eukaryotes (Kim et al., 1997), the main focus of this study. Therefore, we consider here two different mechanisms allowing the achievement of precise adaptation downstream of the receptor in a signaling pathway.

The scheme leading to precise adaptation proposed here is based on the assumption that a signal *S* increases the concentration of an activator *A*, whose action is to convert some response element *R* into the activated form *R** (Fig. 1). For adaptation to take place, an inactivator *I*, mediating the reverse conversion of *R** to *R*, needs to be introduced. *S* activates both *A* and *I* in fixed proportion. As shown in the Appendix, this scheme can lead to perfect adaptation because the corresponding equations have solutions for the concentration of *R** that are not a function of *S*. Formulation of these equations requires further assumptions, namely that the reactions of activation (production) of *A* and of *I* have the same form of dependence on *S*. A similar scheme achieving perfect adaptation (not shown) can be formulated relying on the inactivation of *I* being a saturated process. Below, we show that these two mechanisms represent plausible descriptions of the biochemical processes underlying gradient sensing in amoebae and neutrophils. In Fig. 1 *B* we demonstrate numerically that the scheme in Fig. 1 *A* leads to perfect adaptation to changes in the external signal *S*. The model equations for this and the other simulations are found in the Appendix. The amplitude and duration of the response is a function of the ratio of inactivation rates of the activator *A* and inactivator *I*. If the activation of *R* is fast compared to the activation of the two enzymes, the concentration of *R** is a function of the ratio of the concentrations of *A* and *I*. The steady-state concentration of *R** is independent of both the external signal concentration and the ratio of inactivation rates. The peak value of the transient response is inversely proportional to the adaptation time.

Possible mechanisms of signal amplification (gain in signaling)

Significant nonlinear signal amplification has been postulated to occur in the biochemical pathways mediating eukaryotic gradient sensing. As discussed above, this phenomenon appears to be so dramatic that previous modeling efforts have been focused primarily on description of the high gain rather than adaptation aspects of the sensory signal transduction. Moreover, the presence of a Turing-like positive feedback mechanism is often assumed. However, as mentioned above, the Turing mechanism is not particularly appealing as a means for amplification in gradient sensing. Here, we propose a different amplification scheme, also based on a positive feedback loop.

The overall rate of an enzymatic reaction far from saturation with a given reaction efficiency (measured as the ratio of the maximum rate to the Michaelis constant, v_{max}/K_M) can be increased if the concentration of the active enzyme or that of the substrate is augmented. In the feedback scheme we propose (Fig. 2 *B*), the reaction product *R** affects the supply of the substrate *R*, but not the activation of the enzyme. The supply here can mean regulation of a reaction resulting in production of *R* or a transport process leading to increased local concentrations of *R*. The concentration of the active enzyme is taken to be proportional to the external signal *S*. If the signal is absent, the reaction cannot proceed and the positive feedback, if present, is discontinued. If the signal is present, the reaction proceeds, and the substrate-supply feedback gets activated. This sort of positive feedback is inherently dependent on the presence of the external signal. It is important to emphasize that the positive feedback-containing scheme presented in Fig. 2 *B*, unlike other mechanisms involving positive feedback (such as that in Meinhardt, 1999), allows the sensory system to be sensitive to variations of extracellular signal strength. Indeed, this scheme includes a reaction that can only proceed in the presence of external signal activation. Therefore, the feedback loop in Fig. 2 *B* contains a sort of a circuit breaker that allows the system to avoid going into signal-independent auto-activation cycling mode. As soon as the external signal is removed (or the system has adapted to it) the positive feedback is inactivated.

In principle, signal amplification does not need to involve a positive feedback as a mechanism. For instance, amplification may occur due to high cooperativity of the activation process or because not only the concentration of the product (*R**) but also that of the substrate (*R*) are positively regu-

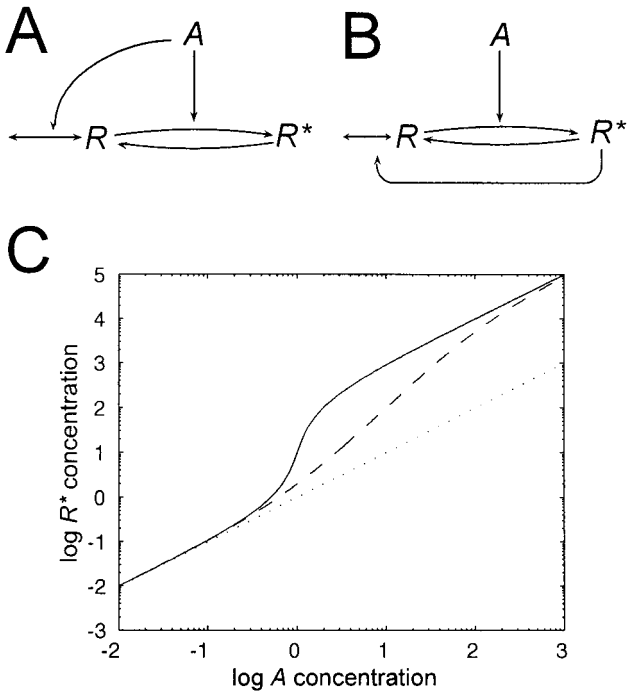

FIGURE 2 Possible mechanisms for signal amplification. (*A*) Nonlinear signal amplification can be achieved by having the activation process act at multiple levels as in A, where the enzyme catalyzes the activation of both the response element R^* and its substrate R. (*B*) Stronger amplification is achieved through the "substrate supply" mechanism of positive feedback in which the response element acts to increase the concentration of its precursor. (*C*) Input–output response of the systems depicted in (*A*) (*dashed line*) and (*B*) (*solid line*). For comparison, the case when the signal A acts only on the conversion from R to R^* with no positive feedback is shown (*dotted line*). As discussed in the text, for small and large concentrations of A, the two systems in (*A*) and (*B*) exhibit the same slope and thus have the same gain. However, for intermediate concentrations of A, the positive feedback scheme exhibits much higher slopes. Constants used are $\alpha = 100$, $\beta = 100$, $\gamma = 1$, $\delta = 10$, $\epsilon = 0$ (*dashed*) and $\alpha = 100$, $\beta = 100$, $\gamma = 1$, $\delta = 0$, $\epsilon = 10$ (*solid*).

lated by the signal S (Fig. 2 *A*). Although simulations corresponding to both these schemes show a nonlinear response to changes in the input levels, the positive feedback-mediated scheme shown in Fig. 2 *B* can provide far higher gains. We can expect, therefore, that, in systems exhibiting high-gain behavior, as many gradient sensing systems seem to do, the positive feedback outlined in Fig. 2 *B* will be present in one way or another.

Provided that the inactivator acts to reverse the processes mediated by A, the possible amplification schemes in Fig. 2 can be combined with the adaptation scheme proposed in Fig. 1 to obtain high-gain signaling with perfect adaptation (Fig. 3). It is thus possible to achieve both adaptation and amplification properties on the same level in a sensory signaling pathway (conversion of R into R^* and the reverse process).

Adaptation and amplification may also occur on different levels. For example, in the two-step pathway shown in Fig. 3 *B*, adaptation occurs on the level of R^*, whereas amplification takes place one step downstream, on the level of R_1^*. Placing adaptation upstream of the gain-producing processes may be advantageous if the same upstream signal activates several downstream pathways. Each of those pathways may have different amplification mechanisms and characteristics, but all cease activation as soon as adaptation in a single upstream reaction takes place. We will discuss below a possible relevance of this argument to various G-protein-mediated signaling processes in eukaryotic gradient sensing.

Persistent signaling in the presence of ligand gradients: gradient sensing

In the previous sections, we analyzed how G-protein-activated signaling systems can adapt perfectly to spatially homogeneous changes in ligand concentration. The same systems become activated persistently in the presence of ligand gradients. It is of interest, then, to see whether the simple schemes presented above are sufficient to explain both adaptability and persistent signaling depending on the spatial organization of the input signal. If we assume all intracellular signaling to occur locally (e.g., within a close neighborhood of the receptor–G-protein complex), perfect adaptation would mean that signaling activity would tend to the same steady-state value independent of the local extracellular ligand concentration. Therefore, the assumption of local signal transduction in combination with perfect adaptation does not allow formation of a gradient of intracellular signaling activity even in the presence of an external ligand gradient. It follows that some aspect of signaling has to be global (diffusible) within the cytosol. Additional analysis reveals (data not shown) that the highest activity gradient results if the inactivator is allowed to diffuse while the activator A is assumed to be immobile or slowly diffusing (see also Postma and van Haastert, 2001). This assumption is sufficient to predict both adaptability and persistent signaling, as illustrated in Fig. 3. In Fig. 3, *C* and *D*, we illustrate the gain amplification of the positive feedback-containing scheme depicted in Fig. 3 *B* and its gradient-sensing capabilities. The only signaling molecule that is allowed to diffuse is the inactivator. At first, the system is excited by a homogeneous change in external source—all parts of the cell experience the same activation levels. At a later point, the levels of R^* (Fig. 3 *C*) and R_1^* (Fig. 3 *D*) adapt to the signal. Note, however, that the increase in concentration for R_1^* is considerably larger. The system is then excited by a spatially inhomogeneous signal. The concentration of S at the "front" is increased by 5% and that of the "rear" is decreased by 5% with corresponding changes linearly along the length of the cell. The system now exhibits a corresponding graded response. Note that, once again, the increase in activity of R_1^* is considerably larger

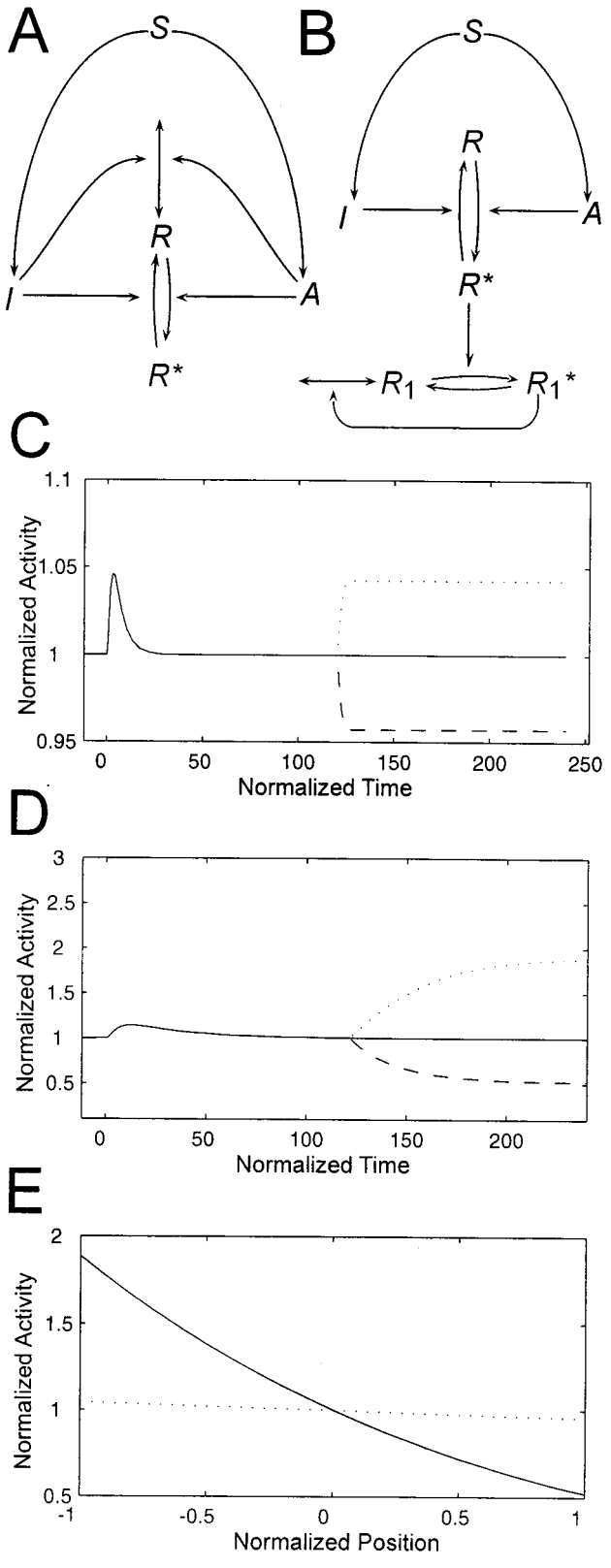

FIGURE 3 Integrated adaptation and signal amplification schemes. (*A*) The adaptation scheme of Fig. 1 can be combined with the amplification schemes of Fig. 2 at the same level. This scheme is similar to that of Fig. 1 *A*, but, in this case, the activation enzyme also increases the concentration of the substrate *R*. Provided that the activation of the two enzymes *A* and *I* by the external signal *S* is proportional, the system will adapt, but the transients will be amplified compared to Fig. 1 *A*. (*B*) The schemes can also be combined in series. Here the adaptation scheme of Fig. 1 *A* is followed by the signal amplification scheme of Fig. 2 *B*. The effectiveness of the latter scheme is illustrated by plotting the corresponding concentrations of R^* (*C*) and R_1^* (*D*). In these figures, a one-dimensional model of the cell's response is simulated. At 0 s, the concentration of *S* is increased uniformly by 10%. As can be seen, the peak increase in the concentration of R_1^* is significantly higher than that of R^*. When the external signal becomes nonhomogeneous, this has significant implications to the cell's polarization. At 120 s, the external concentration is increased 5% at the front and decreased 5% at the rear. In Fig. 3 *C* and *D*, we show the concentrations at the front (*dotted*), center (*solid*), and rear (*dashed*). (*E*) The concentrations at steady state (240 s) across the normalized length of the cell. The normalized concentrations of R^* (*dotted*) and R_1^* (*solid*) are plotted. As expected from Eq. A8 in the text, the $\pm 5\%$ external gradient in *S* manifests itself in a smaller gradient for R^*. However, because this concentration is near the point of highest gain in the second subsystem, a large concentration gradient in R_1^* ensues.

and displays nonlinearity of response. The equilibrium responses in both R^* and R_1^* along the length of the cell are contrasted in Fig. 3 *E*.

G-protein-mediated gradient sensing: relationship between the model and biochemistry

In this section, we consider the known biochemistry of eukaryotic gradient sensing based on activation of G-protein-associated chemokine receptors (G_i family of G-proteins), as studied in *D. discoideum* and neutrophils. The principal signaling pathways, shown to be essential in a variety of experiments, are illustrated in Fig. 4 *A*. Receptor occupation by a chemoattractant leads to G-protein activation followed by activation of various downstream effectors, most notably phosphatidylinositol 3-kinase-γ (PI3K) (Rickert et al., 2000). Activation of PI3K leads to phosphorylation of various phosphoinositides at the D-3 position of the inositol ring. Phosphoinositide phosphates PI(4,5)P_2 and PI(3,4,5)P_3 (henceforth denoted P_2 and P_3, respectively) can further transduce the signal by providing binding sites for various downstream PH-domain-containing signaling components, such as PLCδ, AKT, and CRAC (Parent and Devreotes, 1999; Servant et al., 2000). A variety of PH-domain-containing markers has been developed allowing for straightforward monitoring of phosphoinositide formation by observing changes in membrane-associated fluorescence. Thus, phosphoinositide concentrations are commonly used as readouts of chemoattractant-stimulated signal transduction. Concentrations of these molecules will also be used as signaling outputs in our analysis.

Another signal-transduction molecule activated by G_i, and capable of affecting phosphoinositide levels in response to chemoattractants, is PLC (specifically $\beta 2$ and $\beta 3$ isoforms) (see Wu et al., 2000 for a summary of recent results).

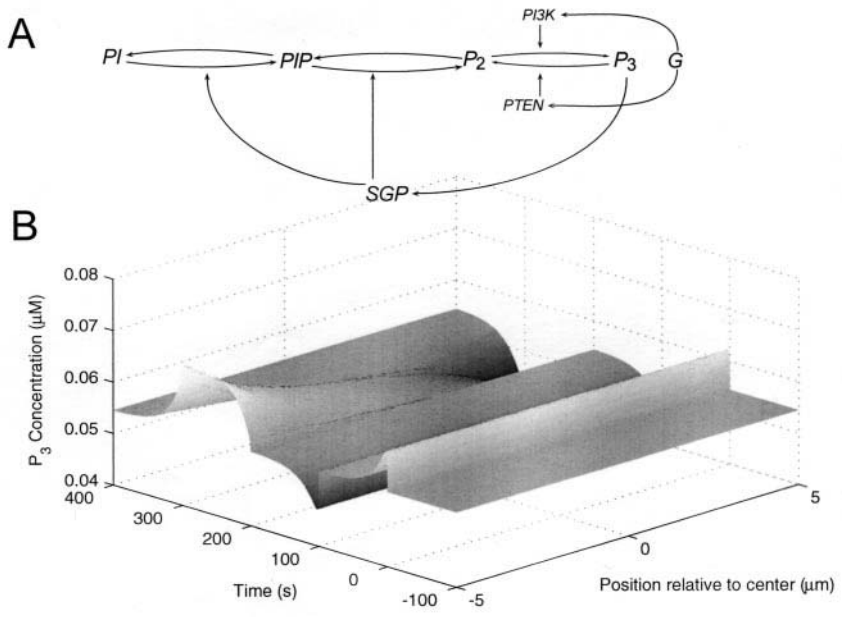

FIGURE 4 Spatial sensing mechanism of *Dictyostelium* and neutrophils. (*A*) The essential biochemical pathways implicated in gradient sensing (described in detail in the text). The output of the pathway is the concentrations of P_3. The nonlinear character of response is assumed to be mediated by one or more small G-proteins (SGP). This feedback is of the substrate supply kind, illustrated in Fig. 2 *B*. (*B*) Simulation of the model corresponding to (*A*). Concentration of P_3 is shown both as a function of time and position along the cell. The signal is increased homogeneously by 20% at 0 s and removed at 100 s. It is seen that the system adapts perfectly both these changes. A graded input is applied (+5% at the front, −5% at the rear and varying linearly along the length of the cell) at 200 s. The graded response in P_3 concentration, which disappears after removal of the graded input at 300 s, is shown.

PLC acts by hydrolyzing P_2 to insosytol-3-phosphaste and diacylglycerol, both of which may affect downstream signaling events, including Ca^{2+} upregulation and activation of protein kinase C (PKC). It may appear that chemotactic events can be influenced negatively by PLC activation, because the P_2, the substrate for PI3K, is depleted. Experimental evidence shows that depletion of PLC can indeed affect chemotaxis positively for some chemoattractants, but has no significant effect on chemotaxis toward other chemoattractants. The effect of PLC is thus not uniform throughout chemoattractant-receptor families and is probably receptor specific. In particular, it has been suggested that PLC activation leads to downregulation of signaling by certain receptor classes by receptor desensitization through activation of PKC (Ali et al., 1999). In this report, we assume that, although PLC may affect P_2 concentration to some degree, this effect is insignificant for the signaling pathways involved in gradient sensing.

Numerous studies indicate that plasma-membrane concentrations of P_3 is relatively low in the absence of stimulation and return precisely to the baseline values following spatially uniform changes in ligand concentration (perfect adaptation). The total cellular and possibly cell membrane concentration of P_2, in contrast, is relatively high in the absence of the signal and does not seem to change significantly following exposure to chemoattractant (Stephens et al., 2000). However, a wealth of data indicates that P_2 induces uncapping and subsequent elongation of actin filaments by modulating interaction of profilin, α-actinin, vinculin, talin, and various actin-capping proteins with actin (Czech, 2000). These findings suggest a possibility of significant local changes in concentration of this phosphoinositide that might be masked when compared to its total cellular concentration. A recent study provides support for this view (Tall et al., 2000). Finally, the baseline concentration of PI(4)P (denoted here as PIP) is relatively high,

TABLE 1 Kinetic rate constants assumed in simulation in Fig. 4 *B*

$k_{-K} = 5.0\ s^{-1}$	$k_K = 5.0\ s^{-1}$	
$k_{-P} = 0.57\ s^{-1}$	$k_P = 0.49\ s^{-1}$	
$k_{-S} = 2.1\ s^{-1}$	$k_S = 8.0\ s^{-1}$	$D = 5\ \mu m^2\ s^{-1}$
$k_{-1} = 2.1\ s^{-1}$	$k_1 = 1.0 \times 10^3\ \mu M\ s^{-1}$	$k_{11} = 1.4\ s^{-1}$
$k_{-2} = 1.4\ s^{-1}$	$k_2 = 6.2 \times 10^{-4}\ s^{-1}$	$k_{21} = 4.3\ \mu M^{-1}\ s^{-1}$
$k_{-3} = 5.0\ \mu M^{-1}\ s^{-1}$	$k_3 = 8.0 \times 10^{-2}\ \mu M^{-1}\ s^{-1}$	$k_{31} = 2.9 \times 10^{-3}\ \mu M^{-1}$

whereas its regulation during signal transduction is not well understood (Stephens et al., 2000).

As indicated in Fig. 4 *A*, phosphoinositide regulation may involve a number of positive feedback mechanisms. It is well documented, for example, that activity of PIP5Ks, the enzymes acting to form P_2 from PIP, is positively regulated by small G-proteins Rac, Rho, and Arf (Czech, 2000). These proteins, in turn, can be upregulated through formation of P_3 (Missy et al., 1998). Significantly, formation of PIP in the Golgi complex can be positively regulated by Arf through recruitment of phosphatidylinositol-4-OH kinase (PI4K) (Czech, 2000). It is conceivable that similar upregulation of PIP in the plasma membrane may occur through the action of Rho and Rac. The resultant high concentrations of PIP will provide more substrate for formation of P_3 (through increased P_2 formation). Finally, a significant role of Cdc42 activation by phosphoinositides in response to a chemoattractant has been suggested by recent experiments (Glogauer et al., 2000). Again, this small G-protein may, by analogy with Rac, Rho, and Arf be involved in the biochemical positive feedback proposed here.

The perfect adaptation of P_3 is of central importance to our model. Initially, it was suggested that adaptation took place primarily at the level of receptor by feedback phosphorylation of its C-terminal cytoplasmic domain following signal propagation (Knox et al., 1986). However, as mentioned above, receptor modification is not necessary for adaptation, and additional mechanisms underlying this property must exist (Kim et al., 1997). In the following discussion, we assume that the chemoattractant receptor is modified to prevent phosphorylation. From Fig. 4 *A*, it can be seen that the only remaining possibilities are to assume that either adaptation of the receptor-associated G-protein, or that the formation of P_3 adapts to changes in signaling input. Although perfect adaptation at the level of G-protein seems attractive for explanation of a variety of G-protein-activated processes (both phosphoinositide-dependent and not) exhibiting precise adaptation, there are experimental indications that no such adaptation takes place. First, preincubation of *D. discoideum* cells with the chemoattractant cAMP decreases the ability of the G-protein to be activated by a GTP analog in a receptor-independent manner (Pupillo et al., 1992). Second, FRET studies of dissociation of α and $\beta\gamma$ subunits of G-protein occurring in G-protein activation reveal that these subunits remain dissociated as long as the receptor is occupied (Janetopoulos et al., 2001). These findings indicate that G-protein remains activated continuously in the presence of the signal, making it likely that adaptation occurs downstream of G-protein activation.

Assuming that adaptation takes place downstream of G-protein activation, this implies that activation of the G-protein and its effectors including PI3K remains elevated as long as the ligand is present. Because the level of P_3 adapts perfectly, a phosphatase opposing PI3K, most likely PTEN, has to be upregulated in response to G-protein activation. Currently, we do not know precisely the mechanism of PTEN activation and thus cannot assert the identity of the P_3 inhibitor. However, we can predict, on the basis of the above considerations, that this inactivator is either regulated directly by the receptor or G-protein in a manner similar to activation of PI3K, or is activated by its substrates, e.g., P_3. In the latter case, we also predict that inactivation of this phosphatase is a saturated process. Regulation of the inactivator enzyme by the substrates appears to be less likely, because no adaptation occurs when P_3 is produced by means other than G-protein-mediated signaling, e.g., by insulin or PDGF receptor activation (Oatey et al., 1999). Adaptation is thus likely to be dependent on the events upstream of phosphoinositide metabolism.

As discussed above, to account for persistent signaling in the presence of chemoattractant gradients, candidates for inactivator molecules (PTEN or similar molecular species) have to possess an additional property. Namely, the inactivator molecule has to be diffusible in its active state. Members of PTEN families have this property, and can be considered as relevant contenders for the role of inhibitor.

The issue of signal amplification in the biochemical pathways defined above can now be addressed. We mentioned that there are feedback mechanisms mediated by the small GTPases of the Rho family that can increase the production of P_2 and PIP following upregulation of P_3. Because P_2 and PIP are substrates required to produce P_3, the amplification can proceed according to the gain mechanisms described above (Fig. 2). Indeed, production of P_3 is amplified by the positive feedback from P_3 directly onto formation of its substrate P_2. Here the activator A is PI3K, whereas the substrate R is P_2 and the product R^* is P_3. In both cases, the activation ceases as soon as the activator (the active PI3K) is removed. These gain schemes are therefore sensitive to signal variations (including changes in the ligand gradients) and can operate successfully if adaptation occurs at the level upstream of phosphoinositides. As illustrated above, these schemes are also compatible with the adaptation mechanisms operating at the level of phosphoinositides.

From the above consideration, the following likely scheme of G-protein-mediated signal transduction events in *D. discoideum* and neutrophils in response to chemoattractants emerges. Following G-protein activation of PI3K, this enzyme increases the concentration of P_3. Following this initial increase, one or more members of the Rho family of small G-proteins is activated, leading to upregulation of membrane-localized PIP5K and PI4K. These kinases, in turn, increase production of PI3K substrates: P_2 and PIP, leading to signal amplification. The G-protein activation also leads to activation of PTEN or a similar PI3K-counteracting phosphatase. As a result, in spatially uniform concentrations of the ligand, the action of PI3K is balanced to achieve the baseline levels of D-3-position inositol phosphorylation. The feedback loops are interrupted and the signaling mechanism adapts perfectly. If the system is faced

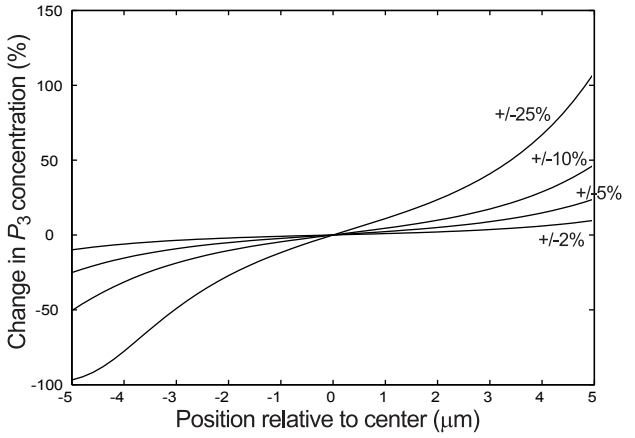

FIGURE 5 Spatial sensing mechanism: response to various external gradients. The system of Fig. 4 was subjected to varying gradients, ±2%, ±5%, ±10%, and ±25%, relative to that of the center, in the concentration of the external source. The spatial response along the length of the cell is plotted.

TABLE 2 Sensitivity analysis

	Gradient			Gradient	
	Decrease (%)	Increase (%)		Decrease (%)	Increase (%)
k_{-K}	5.1	5.4	k_1	5.4	5.2
k_K	5.4	5.1	k_{11}	65.1	65.0
k_{-P}	9.9	2.2	k_{-2}	5.1	5.4
k_P	5.1	5.4	k_2	66.2	60.4
D	24.5	154.9	k_{21}	5.4	5.1
k_{-S}	5.1	5.4	k_{-3}	5.1	5.4
k_S	5.4	5.1	k_3	5.0	5.0
k_{-1}	5.1	5.4	k_{31}	67.0	60.8

Nominal parameter values were either increased or decreased five-fold. The observed gradient, defined as the ratio P_3(front)/P_3(rear) − 1, was computed. The nominal value is 65.1%. From the numbers obtained, it can be seen that deviations away from the nominal parameter values cause a loss in the ultrasensitivity of the system (see text).

with a chemoattractant gradient, diffusion of PTEN or a similar inactivator leads to an incomplete balance of PI3K action and results in persistent signaling oriented in the direction of the gradient.

The mathematical description of our model of the adaptation mechanism of *D. discoideum* and neutrophils is found in the Appendix, and the results of corresponding simulations are shown in Fig. 4 *B*. The kinetic constants used are given in Table 1. The homogeneous concentration of G-protein signal was first increased by 20% from its baseline level at $t = 0$ s. This results in a perfectly adapting spatially homogeneous response. This response is duplicated when the G-protein signal returns to basal level (100 s). Finally, a graded input is applied (200 s) by a graded level of G-protein signal varying from the basal level +5% at the front and −5% at the rear and linearly throughout the cell. Our model exhibits a graded response, with the ratio activity between front and rear nearing ±25% that disappears when the G-protein signal once again returns to the basal level (300 s).

Although the responses seen in Fig. 4 *B* are highly nonlinear, their amplitudes are not as great as may be expected on the basis of experimental data, often showing what apparently are more substantial increases. However, the experiments are often performed with gradients not as shallow as the ±5% gradient assumed in Fig. 4 *B*. To explore the response characteristics of the system depicted in Fig. 4 further, we subjected the cell model to different gradients of the G-protein, varying from ±2% to 25% (Fig. 5). It can be easily seen that the intracellular activity gradient is a sensitive nonlinear function of the gradient value. In particular, there is a more than two-fold increase in activity at the cell front in the ±25% gradient. This result is important, because it shows that the system in Fig. 4 can respond to the value of the gradient, not just the presence versus absence of gradient. The relatively low response seen for small gradient values is consistent with low precision of gradient detection seen in cells migrating in shallow chemoattractant gradients. The precision goes up as the gradient values increase.

To measure the system's sensitivity to parameter variations, each kinetic constant was increased/decreased five-fold. The response was checked for two qualitative properties. First, does the system adapt? To determine this, we calculated the concentration just before 100 s to just before 0 s. We found that, in all cases, the difference between these two concentrations amounted to <0.2%. Thus, perfect adaptation is a structural property of the model, not unlike that in Barkai and Leibler (1997). Second, we determined whether the system can detect spatial gradients. For this, we compute the activity ratio between front and rear of the cells at 300 s. The respective changes are seen in Table 2. From these data, it is clear that large deviations from most of the nominal kinetic parameters can cause a loss of the ultrasensitivity obtained. This can be explained by analogy to the gain mechanism depicted in Fig. 2 *B* and analyzed in the Appendix. In particular, a relative-large increase in internal gradient is achieved if the input concentration is centered at the "transition" regime of the system in Fig. 2 *B*. In Fig. 2 *C*, this amounts to $\log A = 0$. This means that a small relative difference between front and rear in the concentrations of this stimulus will cause a large relative difference in the response.

However, if the kinetic parameters deviate from their nominal values, the regime of operation will shift either to the right or left on Fig. 2 *C*, where the slope (log R* versus log A) is ~1. Thus, the internal gradient will mirror the external gradient. We thus conclude that the property of spatial sensing, like that of adaptation, is robust, but that the ultrasensitivity seen is not.

DISCUSSION

In this study, we argue that substantial insights into the problem of eukaryotic gradient sensing can be gained from mathematical analysis of the necessary conditions for some of the biochemical properties of this process. Namely, any proposed biochemically-based model has to be able to account for both perfect adaptation of signaling to spatially homogeneous variations of chemoattractant concentration and also for high-gain persistent polarized signaling in response to chemoattractant gradients. The model also needs to be able to predict a high degree of sensitivity of polarized signaling to changes in the ligand gradient, e.g., due to gradual changes in the value or direction of the gradients. As demonstrated here, these necessary conditions substantially limit the number of possible ways a gradient-sensing biochemical network can be organized. The mathematically motivated limitations, coupled with information on various aspects of known biochemistry, allowed us to suggest a plausible scheme of gradient sensing in *D. discoideum* and neutrophils.

First, we considered the property of perfect adaptation. Perfect adaptation is commonly observed in various G-protein or growth-factor receptor-mediated signaling pathways implicated in gradient sensing. Several models of perfect adaptation in these pathways have been suggested before. For example, in Tang and Othmer (1994), it is proposed that adaptation occurs due to activation of both activating and inhibitory G-proteins. Other investigators ascribed adaptation mechanism to receptor regulation properties (Knox et al., 1986). We also should note that a receptor modification-based model has been successfully advocated for bacterial chemotaxis (Alon et al., 1999). Here, we investigate two models distinct from those proposed previously primarily because recent experimental observations add new restrictions on how a biochemical scheme underlying adaptation can operate. In particular, it has been determined that receptor phosphorylation is not essential in adaptation and that no redistribution of receptor molecules occurs in migrating *Dictyostelium* cells (Kim et al., 1997). In addition, only one G-protein species has been shown to mediate adaptation and chemotaxis (Neptune and Bourne, 1997), which argues against a previously proposed model of G-protein-based adaptation (Tang and Othmer, 1994).

The adaptation schemes proposed here postulate, in general, the existence of a process, the regulation of which results in adaptation of the activity of this process with respect to an external stimulus. The possible adaptation in activity of the G-protein to activation of the associated receptor or adaptation of phosphoinositide phosphorylation can be considered as examples of this process. As down-regulation of activation is presumed to be mediated by an inhibitory molecule, assumptions on how the inactivator itself is activated need to be made. Two possibilities can then be considered: inactivator regulation by the activity of the process itself or by events upstream of the process. The fact that adaptation is perfect leads to further limitations on the mechanisms of inactivator regulation. In particular, if the inactivator is regulated downstream of the adaptation process, the inactivator downregulation has to be saturated. If, however, an upstream process regulates the inactivator, this regulation needs to be proportional to the activation of the corresponding activator. These conditions for perfect adaptation can be tested experimentally. In particular, on the basis of the plausible biochemical scheme proposed in the text, one can predict that the steady-state activation of PTEN or a similar phosphatase is proportional to activation of PI3K. Further analysis of PTEN regulation is needed to verify this prediction.

Another prediction concerning the inactivator is that it has to be freely diffusible in the cytosol. This prediction reflects an added necessary condition needed to explain persistent signaling polarization in chemoattractant gradients in addition to perfect adaptation to spatially homogeneous changes in chemoattractant. Again, for PTEN or other inactivator candidate, this prediction can be verified experimentally. For instance, any PTEN modification preventing its diffusion is likely to limit the accuracy of gradient detection in chemotaxis. It is important to emphasize that the predictions as to the nature of the inactivator regulation and its diffusivity are made on the basis of consideration of the basic properties of perfect adaptation and persistent signaling and, thus, are expected to hold for any candidate for the role of the inhibitor.

A major challenge in modeling gradient sensing is to reconcile the strongly nonlinear signal response with high sensitivity to the presence and the amplitude of the signal. So far, it has been common to assume that some sort of Turing-like positive feedback acting from the activator of signaling onto its own production is needed to explain the high gain characteristics of signal amplification. This hypothesis, however, invariably leads to formation of stable signaling patterns independent of the external ligand gradient. We argue here that several alternative schemes, with only one relying on a positive feedback, can be proposed to explain nonlinear signal amplification. Furthermore, there is a significant difference between the nature of the positive feedback mechanism proposed here and the modification of the Turing mechanism proposed by Meinhardt and others. The mechanism suggested here postulates that gradient sensing can be mediated by a positive feedback from the activator onto the supply of its precursor (or its inactivated form) rather than on the activator production itself. This kind of "substrate supply"-driven feedback scheme provides an opportunity to amplify the response significantly, while retaining the sensitivity to the presence of the promoter-activating enzyme. No requirement for a second inhibitor, as needed in the Meinhardt model, is any longer present. This approach can be used to modify not only the gradient-

sensing signaling schemes suggested before, but also perhaps other models, in which a Turing-like pattern-generating schemes are utilized but not justified.

Consideration of the biochemical mechanisms implicated in gradient sensing in *D. discoideum* can serve to verify the plausibility of a signal gain scheme. Indeed, although Ca^{2+}-induced Ca^{2+} release proposed by Meinhardt has been shown to be dispensable for gradient sensing in *D. discoideum*, phosphorylation of various phosphoinositides is thought to be at the core of the corresponding signal transduction. Here, we propose the existence of a small G-protein-mediated positive feedback scheme leading to production the phosphoinositides P_3. Its concentration, very low in quiescent cells, undergoes sharp transient (in adaptive response) or persistent (in gradient-sensing response) increases following exposure to a chemoattractant. A quick analysis of the available biochemical information on the underlying signal transduction reveals that the mathematical mechanisms suggested for the substrate supply-mediated positive feedback are likely to be embodied in the biochemical mechanisms. The positive feedback can be mediated by upregulation of PIP and P_2 concentrations through the action of one or more small G-proteins (Cdc42, Rac, or Rho), which are, in turn, activated by P_3. Evidence for the importance of small G-protein-mediated feedback in cell orientation has been obtained recently (Rickert et al., 2000).

Although, in this study, we concentrated on modeling of gradient sensing that can occur independently of cell locomotion, in unperturbed chemotactic systems, the influence of various factors omitted from this analysis, such as cytoskeleton-mediated polarization of signaling components, can be of major importance. Indeed, even in the absence of an external gradient, a variety of cells, including *D. discoideum*, can migrate in random directions. These cells are polarized with various signaling molecules, including G-proteins, localized to what can be regarded as the front and the back of the cell (Jin et al., 2000). Polarization of signaling apparatus can create intracellular signaling gradient even in the absence of external chemoattractant gradients. Cytoskeleton-mediated extension of filopodia can further influence the gradient detection by providing the opportunity for temporal gradient sensing, in which gradients are measured by subtracting ligand concentrations detected at different times in the same subcellular location. Numerous questions are still open in this aspect of chemotaxis, such as what causes symmetry breaking in the cytoskeleton architecture leading to cell polarization and how commonly observed oscillations in actin cytoskeleton structure (Vicker, 2000) can influence chemotaxis. This paper provides a "stepping stone" for addressing these questions through an analysis of cytoskeleton-independent gradient-detection mechanisms that can regulate actin polymerization.

We anticipate that, in the further chemotaxis models, the relative roles of P_2 and small G-proteins (Cdc42, Rac, and Rho) in regulation of actin polymerization will be further accounted for. It is becoming clear that actin is polymerized at the leading edge of migrating cells according to the dendritic nucleation model, whereby a regulatory protein complex, Arp2/3, both creates new filaments and cross-links them into a branching meshwork. Recently, it has been shown that costimulation of Arp2/3 by both P_2 and small G-proteins (Cdc42 in particular) through accessory WASP protein family is essential for its activation (Blanchoin et al., 2000). It is important to have congruent activation of both these regulators in formation of cell membrane protrusions at the front of the cell. The nature of the positive feedback signal amplification suggested here guarantees that both P_2 and small G-proteins become activated only if PI3K signaling is present. Unrelated regulatory events leading to increasing concentrations of just P_2 or small G-proteins can mediate other important processes, such as stabilization of potassium channels (Kobrinsky et al., 2000) or membrane reshaping (Loyet et al., 1998) but not formation of spikes or philopodia characteristic of migrating cells.

In this study, we illustrated how the mathematical model of the processes underlying perfect adaptation and reversible signal amplification can be mapped to biochemical signaling networks that became known through experimental studies in amoebae and neutrophils, probably the most common model systems in studies of chemotaxis. It will be of interest to see whether these general mathematical principles will hold for biochemical signaling networks found in other chemotaxing systems. Studies of chemotropism in yeast revealed important differences in the identity of the sensory pathways involved in gradient sensing in *D. discoideum* and *Saccharomyces cerevisiae* (Arkowitz, 1999). For instance, PI3K does not seem to be a major player in yeast gradient sensing, whereas the MAPK Fus3 seems to have an essential role. In addition, in migration of fibroblasts or neuronal growth cones, reception of the signal is not mediated by G-proteins. Despite these biochemical differences, we suggest that the major underlying principles proposed in this study, such as the combination of a mechanism for perfect adaptation with substrate-supply-mediated reversible signal amplification will be at the core of most eukaryotic gradient-sensing systems.

It is of interest to compare our gradient-sensing model with qualitative descriptions suggested before. One of the popular ones, proposed in Parent and Devreotes (1999), is conceptually very similar to the one proposed here in that it assumes that perfect adaptation is mediated by a broadly defined balance of the actions of the activator and inactivator of signaling, whereas the persistent response to gradients is generated by an imbalance of these components due to the inactivator diffusion. However, no particular mechanisms (either mathematical or biochemical) have been proposed and analyzed by the authors, which limited the predictive power of the model. In addition, no clear explanation for the sources of nonlinearity in response has been suggested. The

modeling framework proposed here, both in its general theoretical and its plausible biochemical embodiments, provides more opportunities for direct experimental test and further refinement.

APPENDIX

Description of model from Fig. 1

We assume that the response element is found in both an active, R^*, and an inactive, R, state. Conversion from the inactive to the active state is through the activator enzyme A, whereas inactivation is through the enzyme I.

In Fig. 1 *A*, we presented three reactions, in which a molecule is converted by an activator enzyme into the active state and by an inactivator enzyme into the inactive state. These reaction cycles are assumed for the activator A, the inactivator I, and the response element R. The relationship among these components is as follows. For the reaction of R, the activator is A and the inactivator is I. For the reaction of A, the activator is S (the external signal) and the inactivator is a constitutively active molecule (not denoted). By analogy, I is activated by S, and inhibited constitutively. The consideration of all of these reactions will follow the general treatment in Goldbeter and Koshland (1981).

First, we consider a general set of reactions for the interconversion between the active form W^* and inactive form W of a signaling molecule. With the activation mediated by an enzyme E_1, the enzyme–substrate complex designated as U_1 and association, dissociation, and reaction (catalysis) constants denoted, respectively, as k_{c1}, k_{u1}, and k_{a1}, and with the inactivation mediated by E_2 and the corresponding parameters (k_{c2}, k_{u2}, and k_{a2}), we have,

$$\frac{dW}{dt} = -k_{c1}WE_1 + k_{u1}U_1 + k_{u2}U_2,$$

$$\frac{dU_1}{dt} = k_{c1}WE_1 - (k_{u1} + k_{a1})U_1,$$

$$\frac{dW^*}{dt} = -k_{c2}W^*E_2 + k_{u2}U_2 + k_{a1}U_1,$$

$$\frac{dU_2}{dt} = k_{c2}W^*E_2 - (k_{u2} + k_{a2})U_2. \tag{A1}$$

It is usual to derive the Michaelis–Menten kinetics from the quasi-steady-state approximation, in which it is assumed that a fast steady state for intermediate enzyme–substrate complexes is achieved ($dU_1/dt = dU_2/dt = 0$). Using these conditions, the equation for the rate of change in W^* given above can be rewritten as

$$\frac{dW^*}{dt} = -k_{c2}W^*E_2 + k_{u2}\frac{W^*E_2}{K_{M2}} + k_{a1}\frac{WE_1}{K_{M1}}$$

$$= -\delta W^*E_2 + \lambda WE_1. \tag{A2}$$

If both enzymes E_1 and E_2 operate far from saturation, we can assume that the values for these enzymes given in Eq. A2 correspond to the total rather than free concentrations. We will use this form for describing the particular reactions for R, A, and I. The reaction for R is thus

$$\frac{dR^*}{dt} = -k_{-R}IR^* + k_RAR.$$

As mentioned above, we assume that the activating and inhibitory enzymes also occur in two states: active (A and I) and inactive. The total concentrations of these two enzymes are A_{tot} and I_{tot}, respectively. A third enzyme, the external signal S, mediates activation of two enzymes, whereas inactivation is assumed to be constitutive. Again, using the form Eq. A1, the differential equations describing the active states can be written as

$$\frac{dA}{dt} = -k_{-A}A + k'_AS(A_{tot} - A),$$

$$\frac{dI}{dt} = -k_{-I}I + k'_IS(I_{tot} - I).$$

Moreover, we assume that the inactivating reactions for both A and I are far more efficient (as measured by the value of the ratio of the catalytic rate constant and the Michaelis–Menten constant) than the activating reaction mediated by S. A result of this assumption is that the available substrate for S far exceeds the concentration of the two enzymes; i.e., $A_{tot} \gg A$ and $I_{tot} \gg I$, so that these equations can be simplified as

$$\frac{dA}{dt} = -k_{-A}A + k_AS, \tag{A3a}$$

$$\frac{dI}{dt} = -k_{-I}I + k'_IS, \tag{A3b}$$

where $k_A = k'_AA_{tot}$ and $k_I = k'_I I_{tot}$. We can rewrite these equations using the dimensionless fraction of active molecules $r = R^*/R_{tot}$, dimensionless time $\tau = k_{-a}t$, and similarly, dimensionless concentrations: $a = (k_R/k_{-A})A$, $i = (k_Rk_Ak_{-I}/k_Ik^2_A)\ I$, and $s = (k_Ak_R/k^2_{-A})S$. The new dimensionless equations are

$$\frac{da}{d\tau} = -(a - s), \tag{A4a}$$

$$\frac{di}{d\tau} = -\alpha(i - s), \tag{A4b}$$

$$\frac{dr}{d\tau} = -\beta ir + a(1 - r), \tag{A4c}$$

where $\alpha = (k_{-I}/k_{-A})$ and $\beta = [(k_{-R}/k_R)(k_{-A}/k_A)]/(k_{-I}/k_I)$. At the steady state, the concentrations of normalized activator and inactivator are both equal to that of the signaling molecule s. For any value of $s > 0$, the normalized concentration of the active response element is

$$r_{ss} = \frac{a/i}{a/i + \beta}, \tag{A5}$$

and we note that it is the ratio of enzyme concentrations that determines the steady-state value of the activity, and that r_{ss} is independent of the concentration of the signal s. Moreover, it is the ratio of inactivation constants α that determines the magnitude of the transient. For $\alpha < 1$ (resp. $\alpha > 1$) activation of A is faster (resp. slower) than that of I and, hence a transient increase (resp. decrease) in the concentration of r results to a positive increase in the concentration of s. When the concentration of the signaling molecule, s, is zero, Eqs. A4 have an arbitrary equilibrium value for the concentration of the active response element r_{ss}. However, to maintain continuity in the steady-state value of r_{ss}, we postulate that the only sensible value is that given by Eq. A5.

To contrast the scheme proposed here with that of Goldbeter and Koshland (1981), we note that, in their study, the equations governing the activation of the two enzymes occurs in the saturating region of Michaelis–Menten kinetics. Based on this assumption, they obtain "ultrasensitivity" in the steady-state response element R^* to changes in the external concentration of S. We consider the opposite regime, in which the enzyme activation

occurs in the linear region of Michaelis–Menten kinetics. Interestingly, the Goldbeter–Koshland model also results in the degree of activation being a function of the ratio of activating and inhibitory enzymes. Therefore, even if we assume a Goldbeter–Koshland-style zero-order-sensitivity regime for R activation, we can still predict perfect adaptation, provided that the concentrations of active A and I depend on S linearly. In this case, there are both adaptation of R^* and amplification of the signal S occurring without any extra mechanisms. Although this scheme may seem attractive for a full description of gradient sensing, a different, positive feedback-based amplification scheme described in the next section agrees better with experimental data (see text).

Description of models from Fig. 2

Both systems can be described by the pair of differential equations;

$$\frac{dR^*}{dt} = -k_{-2}R^* + \frac{k_2AR}{k_M + R},$$

$$\frac{dR}{dt} = -k_{-1}R + (k_1 + k_{1a}A + k_{1*}R^*) + k_{-2}R^* - \frac{k_2AR}{k_M + R}. \quad \text{(A6)}$$

The first equation describes an enzymatic conversion from R to R^* using Michaelis–Menten kinetics, as well as the reverse reaction. In the second equation, we assume that there is a basal level of production of R, with kinetic constant k_1. Two other possibilities exist. If $k_{1a} \neq 0$, then the enzyme A catalyzes the production of substrate as in Fig. 2 A. If $k_{1*} \neq 0$, then R^* provides a positive feedback loop as in Fig. 2 B.

We look for possible equilibria of these two equations. Setting the first equation to zero, one obtains

$$R^* = \frac{k_2}{k_{-2}}\frac{AR}{k_M + R} = \frac{\alpha AR}{\beta + R},$$

where $\alpha = k_2/k_{-2}$ and $\beta = k_M$. Similarly,

$$R = \frac{1}{k_{-1}}(k_1 + k_{1a}A + k_{1*}R^*) =: \gamma + \delta A + \epsilon R^*.$$

Together, these equations lead to the following quadratic equation for the steady-state concentration of R^*:

$$\epsilon(R^*)^2 + (\beta + \gamma + A(\delta - \alpha\epsilon))R^* - \alpha A(\gamma + \delta A) = 0.$$

We consider some special cases in detail. In the base-line level, we assume that $k_{1a} = k_{1*} = 0$; equivalently, $\delta = \epsilon = 0$. In this case, there is only one solution, $R^* = [\alpha\gamma/(\beta+\gamma)]A$, showing that the concentration of R^* increases linearly with that of A.

The situation depicted by Fig. 2 A, where there is no feedback, amounts to setting $\epsilon = 0$. Once again, there is only one solution: $R^* = \alpha A[(\gamma + \delta A)/(\beta + \gamma + \delta A)]$. Notice that, in the two extreme regimes (small and large concentrations of A), the resultant concentration for R^* varies linearly with that of A. For small A, the slope $(\alpha\gamma/(\beta + \gamma))$ is the same as in the previous case. For large A, the slope (α) is strictly larger. In the transition regime, the concentration of R^* varies as the square of A. This is the region when the production of R due to A is now significantly more than the basal level ($k_{1a}A \gg k_1$) but R has not saturated ($k_M \gg R$).

Finally, the third case—that of Fig. 2 B—has $\delta = 0$. Two solutions exist, but only one is non-negative,

$$R^* = \frac{-(\beta + \gamma - A\alpha\epsilon) + \sqrt{(\beta + \gamma - A\alpha\epsilon)^2 + 4\alpha\lambda A}}{2\epsilon}.$$

We first consider the instance where the concentration of A is small, that is, $\beta + \gamma \gg \alpha\epsilon$A. In this instance, the solution matches that of the previous Section. In the other extreme case, where A is very large, the solution approaches $R^* = \alpha$A $+ \gamma/\epsilon$. Thus, asymptotically, this solution matches that of the previous section for large values of concentration in A. The third regime of interest is the "transition," which we describe below.

For the two schemes depicted in Fig. 2 there are three regimes, depending on the concentration of A. When A is small, both schemes give rise to concentrations of R^* that vary linearly with respect to A, and having the same slope. This is the regime when the contributions of either the k_{1a} or k_{1*} terms are small compared to the k_1 term. Thus, neither positive feedback nor the contribution of A on the substrate R is playing a significant role. When $R \gg k_M$, the system saturates. This can only happen when either $k_{1a} \neq 0$ or $k_{1*} \neq 0$. In this regime, more positive feedback or contribution of A on R will not be beneficial, and, therefore, the two schemes have the same slope and, hence, gain.

Where the systems can differ significantly is in the transition area, and we will compare the gains there. To do this, we assume that

$$\gamma \ll R = \gamma + \delta A + \epsilon R^* \ll k_M = \beta.$$

It is straightforward to check that when $\epsilon = 0$, this leads to $R^* = (\alpha\delta/\beta)A^2$. For the positive feedback scheme, in the region far from saturation, $R^* \cong AR/\beta = \alpha A(\epsilon R^* + \gamma)/\beta$. Thus,

$$R^* \approx \frac{\alpha\gamma A}{\beta(1 - \alpha\epsilon A)},$$

provided that $A < 1/(\alpha\epsilon)$. This scheme can provide arbitrarily larger gains near $A = 1/(\alpha\epsilon)$. However, as the concentration of A approaches this threshold, we quickly reach saturation. A comparison of the gains for the two schemes is shown in Fig. 2 C.

Description of models in Fig. 3

We first analyze the model of Fig. 3 A and consider the analysis of the system, assuming that the concentration of the external signaling molecule is homogeneous. This system then combines the schemes of Figs. 1 A and 2 A. The equations governing the evolution of the system are those of Eqs. A3, together with

$$\frac{dR^*}{dt} = -k_{-2}IR^* + k_2AR,$$

$$\frac{dR}{dt} = -k_{-1}IR + k_{1a}A + k_{-2}R^* - k_2AR, \quad \text{(A7)}$$

which is Eq. A2 in the transition regime discussed in the previous section. Analysis of this pair of equations leads to a steady-state concentration value for R^* as in the previous section,

$$R^*_{ss} = \frac{k_2k_{1a}}{k_{-2}k_{-1}}(A/I)^2,$$

so that the steady-state concentration of R^* depends on the square of the ratio of concentrations of A and I.

The system described by Fig. 3 B consists of a cascade of the systems described in Fig. 1 A and the system in Fig. 2 B. Thus, if we once again

concentrate on the transition regime of the previous section, the steady-state concentration of R_1^* is given by

$$R^*_{1-\mathrm{ss}} = \frac{\alpha\gamma(A/I)}{\beta(1 - \alpha\epsilon(A/I))}.$$

We note that it is, once again, the ratio of enzyme concentrations that governs the behavior of the system. When the activity of these enzymes is regulated as in Eqs. A3, constant concentrations of S will lead to steady-state concentrations of the response element that are independent of the level S. This analysis is valid when the system is stimulated by spatially homogeneous source signal concentrations. To account for graded inputs, the system is modified slightly. We assume that the concentrations of all system species are localized except for the inhibitor, which is allowed to diffuse. To account for this diffusion, we modify one term to the differential equation describing the inactivator dynamics, Eq. A3b,

$$\frac{\partial I(t, x)}{\partial t} = -k_{-\mathrm{I}}I(t, x) + k_{\mathrm{I}}S(t, x) + D\nabla^2 I(t, x).$$

For boundary conditions, we assume no flux at either end. Note that the concentration of the inactivator is now indexed according to the spatial dimension.

We model the cell as a one-dimensional system where the concentration of the external signal varies linearly as the spatial parameter x. Thus $S(x) = s_0 + s_1x$. By solving the above equation, the steady-state concentration of the inactivator enzyme can then be calculated as

$$I(x) = \frac{k_{\mathrm{I}}}{k_{-\mathrm{I}}}\left(s_0 + s_1\left(x - \frac{\sinh\sigma x}{\sigma} + \frac{\cosh\sigma x[\cosh\sigma - 1]}{\sigma\sinh\sigma}\right)\right),$$

where $\sigma = \sqrt{k_{-\mathrm{I}}/D}$. Because the activator enzyme cannot diffuse, its steady-state concentration profile mirrors that of the external source, $A(x) = (k_{\mathrm{A}}/k_{\mathrm{A}})S(x)$. Recall that the concentration of the response element is governed by the ratio of these two enzymes, which is now $A(x)/I(x)$, and this equals

$$\frac{A(x)}{I(x)} = \frac{k_{\mathrm{A}}k_{-\mathrm{I}}}{k_{-\mathrm{A}}k_{\mathrm{I}}}\left(1 + \frac{s_1}{s_0 + s_1x} \cdot\left(\frac{\cosh\sigma x[\cosh\sigma - 1]}{\sigma\sinh\sigma} - \frac{\sinh\sigma x}{\sigma}\right)\right)^{-1} < \frac{k_{\mathrm{A}}k_{-\mathrm{I}}}{k_{-\mathrm{A}}k_{\mathrm{I}}}. \quad \text{(A8)}$$

It is the parameter σ that determines the spatial response of the system. For small values of σ, the concentration of $I(x)$ is approximately constant across the length of the cell. Hence, the ratio $A(x)/I(x)$ mirrors that of the external source. When σ is large, the concentration $I(x)$ is linear across the length of the cell, and hence the ratio of $A(x)/I(x)$ is independent of the spatial parameter x.

The output of a simulation involving the system in Fig. 3 *B* is shown in Fig. 3, *C–E*. Parameters used are $k_{\mathrm{A}} = 1\ \mathrm{s}^{-1}$, $k_{-\mathrm{A}} = 1\ \mathrm{s}^{-1}$, $k_{\mathrm{I}} = 0.05\ \mathrm{s}^{-1}$, $k_{-\mathrm{I}} = 0.05\ \mathrm{s}^{-1}$, $k_1 = 1\ \mu\mathrm{M}\ \mathrm{s}^{-1}$, $k_1^* = 100\ \mathrm{s}^{-1}$, $k_{-1} = 1\ \mathrm{s}^{-1}$, $k_2 = 1\ \mu\mathrm{M}^{-1}\ \mathrm{s}^{-1}$, $k_{-2} = 1\ \mathrm{s}^{-1}$, $k_{\mathrm{M}} = 100\ \mu\mathrm{M}$, and $\mathrm{D} = 0.8\ \mu\mathrm{m}^2\ \mathrm{s}^{-1}$. As discussed with regards to the system of Fig. 1 *A*, the property of perfect adaptation does not depend on the value of the parameters chosen. The concentration of the response element R^*, which serves as the output of the first subsystem and input to the second subsystem, has a steady-state value of 1 μM. The other parameter values (k_1, k_1, k_{-1}, k_2, k_{-2}, k_{M}, and D) where chosen to provide large amplification near this operating point. This is achieved by selecting parameters so that the point of highest slope in Fig. 2 *C* matches the concentration of the input of the second subsystem, R^*.

It is seen that the system adapts perfectly to homogeneous changes in the concentration of the external signal S. Graded changes in S lead to graded changes in both the concentrations of R^* and R_1^*. However, as expected from Eq. A8, the relative concentration gradient in R^* is smaller than that of S. However, the amplification subsystem involving R_1^* leads to large gradients in this molecule's concentration, as seen in Fig. 3, *D* and *E*. Varying parameters from these nominal values can have significant effects on the magnitude of the response element R_1^* (not shown).

Description of Model from Fig. 4 A

We assume a one-dimensional model of a cell, 10-μm long. The differential equations describing our model are given below. Except for the following two cases, the reactions are assumed to follow first-order kinetics. First, in the conversion of PI to PIP, and PIP to P_2, the rate constants k_1 and k_2 are augmented by terms proportional to the concentration of the small G-protein; these are meant to express the increase in conversion that is mediated by these proteins. Second, the conversion of P_2 to P_3 follows Michaelis–Mentin quasi-steady-state dynamics. These assumptions lead to the following set of differential equations:

$$\frac{\partial \mathrm{PI3K}}{\partial t} = -k_{-\mathrm{K}}\mathrm{PI3K} + k_{\mathrm{K}}\mathrm{G}$$

$$\frac{\partial \mathrm{PTEN}}{\partial t} = -k_{-\mathrm{P}}\mathrm{PTEN} + k_{\mathrm{P}}\mathrm{G} + D\nabla^2\mathrm{PTEN}$$

$$\frac{\partial \mathrm{SGP}}{\partial t} = -k_{-\mathrm{S}}\mathrm{SGP} + k_{\mathrm{S}}\mathrm{PIP3}$$

$$\frac{\partial \mathrm{PIP}}{\partial t} = -k_{-1}\mathrm{PIP} + (k_1 + k_{11}\mathrm{SGP}) + k_{-2}\mathrm{P}_2 - (k_2 + k_{21}\mathrm{SGP})\mathrm{PIP}$$

$$\frac{\partial \mathrm{P}_2}{\partial t} = -k_{-2}\mathrm{P}_2 + (k_2 + k_2\mathrm{SGP})\mathrm{PIP} + k_{-3}\mathrm{PTEN}\cdot\mathrm{P}_3 - k_3\mathrm{PI3K}\frac{\mathrm{P}_2}{1 + k_{31}\mathrm{P}_2}$$

$$\frac{\partial \mathrm{P}_3}{\partial t} = -k_{-3}\mathrm{PTEN}\cdot\mathrm{P}_3 + k_3\mathrm{PI3K}\frac{\mathrm{P}_2}{1 + k_{31}\mathrm{P}_2}$$

The analysis of this set of equations is similar to that of the previous section. The only difference is that there are now two positive feedback loops. Nevertheless, it is possible to show that, for spatially homogeneous levels of G-protein signaling, the concentration of the signal P_3 is independent on the level of concentration of G. For spatially graded inputs, the spatial distribution of P_3 depends on the spatially local ratio of concentrations of PI3K and PTEN. These spatial distributions are governed as in the previous section. Note, however, that, for these spatially inhomogeneous differences in concentrations to have the greatest effect on the distribution of concentrations of P_3, this ratio must lie in the transition region described in Description of Models from Fig. 2. Kinetic constants used are found in Table 1. These constants were chosen to give basal levels of PIP, P2, and P3 around 50, 30, and 0.05 μM, which is in the range reported (Stenmark, 2000). The diffusion coefficient used corresponds to that predicted in Postma and van Haastert (2001).

The authors gratefully acknowledge P. N. Devreotes, D. Bray, M. D. Levin and D. A. Lauffenburger as well as the anonymous reviewers for their

careful reading of the manuscript and for their helpful insights and suggestions.

Partial support for this work was provided by Burroughs Wellcome Fund's Fellowship in Computational Biology (Interfaces program at Caltech) to A.L., the Whitaker Foundation (P.I.) and the National Science Foundation (P.I.) under grant No. DMS-0083500.

REFERENCES

Ali, H., R. M. Richardson, B. Haribabu, and R. Snyderman. 1999. Chemoattractant receptor cross-desensitization. *J. Biol. Chem.* 274: 6027–6030.

Alon, U., M. G. Surette, N. Barkai, and S. Leibler. 1999. Robustness in bacterial chemotaxis. *Nature.* 397:168–171.

Arkowitz, R. A. 1999. Responding to attraction: chemotaxis and chemotropism in *Dictyostelium* and yeast. *Trends. Cell Biol.* 9:20–27.

Barkai, N., and S. Leibler. 1997. Robustness in simple biochemical networks. *Nature.* 387:913–917.

Blanchoin, L., T. D. Pollard, and R. D. Mullins. 2000. Interactions of ADF/cofilin, Arp2/3 complex, capping protein and profilin in remodeling of branched actin filament networks. *Curr. Biol.* 10:1273–1282.

Czech, M. P. 2000. PIP2 and PIP3: complex roles at the cell surface. *Cell.* 100:603–606.

Eddy, R. J., L. M. Pierini, F. Matsumura, and F. R. Maxfield. 2000. Ca^{2+}-dependent myosin II activation is required for uropod retraction during neutrophil migration. *J. Cell Sci.* 113:1287–1298.

Gierer, A., and H. Meinhardt. 1972. A theory of biological pattern formation. *Kybernetik.* 12:30–39.

Goldbeter, A., and D. E. Koshland. 1981. An amplified sensitivity arising from covalent modification in biological systems. *Proc. Natl. Acad. Sci. U.S.A.* 78:6840–6844.

Glogauer, M., J. Hartwig, and T. Stossel. 2000. Two pathways through Cdc42 couple the *N*-formyl receptor to actin nucleation in permeabilized human neutrophils. *J. Cell Biol.* 150:785–796.

Janetopoulos, C., T. Jin, and P. N. Devreotes. 2001. Receptor-mediated activation of heterotrimeric G-proteins in living cells. *Science.* 291: 2408–2411.

Jin, T., N. Zhang, Y. Long, C. A. Parent, and P. N. Devreotes. 2000. Localization of the G protein $\beta\gamma$ complex in living cells during chemotaxis. *Science.* 287:1034–1036.

Kim, J. Y., R. D. Soede, P. Schaap, R. Valkema, J. A. Borleis, P. J. Van Haastert, P. N. Devreotes, and D. Hereld. 1997. Phosphorylation of chemoattractant receptors is not essential for chemotaxis or termination of G-protein-mediated responses. *J. Biol. Chem.* 272:27313–27318.

Knox, B. E., P. N. Devreotes, A. Goldbeter, and L. A. Segel. 1986. A molecular mechanism for sensory adaptation based on ligand-induced receptor modification. *Proc. Natl. Acad. Sci. U.S.A.* 83:2345–2349.

Kobrinsky, E., T. Mirshahi, H. Zhang, T. Jin, and D. E. Logothetis. 2000. Receptor-mediated hydrolysis of plasma membrane messenger PIP_2 leads to K^+-current desensitization. *Nat. Cell Biol.* 2:507–514.

Loyet, K. M., J. A. Kowalchyk, A. Chaudhary, J. Chen, G. D. Prestwich, and T. F. Martin. 1998. Specific binding of phosphatidylinositol 4,5-bisphosphate to calcium-dependent activator protein for secretion (CAPS), a potential phosphoinositide effector protein for regulated exocytosis. *J. Biol. Chem.* 273:8337–8343.

Meinhardt, H. 1999. Orientation of chemotactic cells and growth cones: models and mechanisms. *J. Cell Sci.* 112:2867–2874.

Missy, K., V. Van Poucke, P. Raynal, C. Viala, G. Mauco, M. Plantavid, H. Chap, and B. Payrastre. 1998. Lipid products of phosphoinositide 3-kinase interact with Rac1 GTPase and stimulate GDP dissociation. *J. Biol. Chem.* 273:30279–30286.

Neptune, E. R., and H. R. Bourne. 1997. Receptors induce chemotaxis by releasing the $\beta\gamma$ subunit of G_i, not by activating G_q or G_s. *Proc. Natl. Acad. Sci. U.S.A.* 94:14489–14494.

Oatey, P. B., K. Venkateswarlu, A. G. Williams, L. M. Fletcher, E. J. Foulstone, P. J. Cullen, and J. M. Tavare. 1999. Confocal imaging of the subcellular distribution of phosphatidylinositol 3,4,5-trisphosphate in insulin- and PDGF-stimulated 3T3–L1 adipocytes. *Biochem. J.* 344: 511–518.

Parent, C. A., and P. N. Devreotes. 1999. A cell's sense of direction. *Science.* 284:765–770.

Postma, M., and P. J. van Haastert. 2001. A diffusion-translocation model for gradient sensing by chemotactic cells. *Biophys. J.* 81:1314–1323.

Pupillo, M., R. Insall, G. S. Pitt, and P. N. Devreotes. 1992. Multiple cyclic AMP receptors are linked to adenylyl cyclase in *Dictyostelium*. *Mol. Biol. Cell.* 3:1229–1234.

Rickert, P., O. D. Weiner, F. Wang, H. R. Bourne, and G. Servant. 2000. Leukocytes navigate by compass: roles of PI3Kγ and its lipid products. *Trends. Cell Biol.* 10:466–473.

Servant, G., O. D. Weiner, P. Herzmark, T. Balla, J. W. Sedat, and H. R. Bourne. 2000. Polarization of chemoattractant receptor signaling during neutrophil chemotaxis. *Science.* 287:1037–1040.

Stenmark, H. 2000. Phosphatidylinositol 3-kinase and membrane trafficking. *In* Biology of Phosphoinositides. S. Cockroft, editor. Oxford University Press, Oxford, UK. 32–108.

Stephens, L., A. McGregor, and P. Hawkins. 2000. Phosphoinositide 3-kinases: regulation by cell surface receptors and function of 3-phosphorylated lipids. *In* Biology of Phosphoinositides. S. Cockroft, editor. Oxford University Press, Oxford, UK. 32–108.

Tall, E. G., I. Spector, S. N. Pentyala, I. Bitter, and M. J. Rebecchi. 2000. Dynamics of phosphatidylinositol 4,5-bisphosphate in actin-rich structures. *Curr. Biol.* 10:743–746.

Tang, Y., and H. G. Othmer. 1994. A G protein-based model of adaptation in *Dictyostelium discoideum*. *Math. Biosci.* 120:25–76.

Traynor, D., J. L. Milne, R. H. Insall, and R. R. Kay. 2000. Ca(2+) signalling is not required for chemotaxis in *Dictyostelium*. *EMBO J.* 19:4846–4854.

Van Duijn, B. and P. J. Van Haastert. 1992. Independent control of locomotion and orientation during *Dictyostelium discoideum* chemotaxis. *J. Cell Sci.* 102:763–768.

Van Haastert, P. J. 1983. Sensory adaptation of *Dictyostelium discoideum* cells to chemotactic signals. *J. Cell Biol.* 96:1559–1565.

Vicker, M. G. 2000. Reaction-diffusion waves of actin filament polymerization/depolymerization in *Dictyostelium* pseudopodium extension and cell locomotion. *Biophys. Chem.* 84:87–98.

Wu, D., C. K. Huang, and H. Jiang. 2000. Roles of phospholipid signaling in chemoattractant-induced responses. *J. Cell Sci.* 113:2935–2940.

Yi, T. M., Y. Huang, M. I. Simon, and J. Doyle. 2000. Robust perfect adaptation in bacterial chemotaxis through integral feedback control. *Proc. Natl. Acad. Sci. U.S.A.* 97:4649–4653.